Anomalously weak influence of source-drain voltage on inelastic scattering processes in quantum Hall systems

Tomoki Machida
CREST, Japan Science and Technology Corporation, Komaba 3-8-1-16-622, Meguro-ku, Tokyo 153-8902, Japan

Susumu Komiyama
Department of Basic Sciences, University of Tokyo, Komaba 3-8-1, Meguro-ku, Tokyo 153-8902, Japan
(Received 11 May 2000)

The inelastic scattering length $L_{\rm in}$ of a two-dimensional electron gas in $Al_{0.3}Ga_{0.7}As/GaAs$ heterostructure crystals at high magnetic fields is studied by analyzing the transition width between quantum Hall plateaus. The dependence of $L_{\rm in}$ on the source-drain voltage $V_{\rm SD}$ is found to be anomalously weak when compared to its dependence on the lattice temperature. The weak $V_{\rm SD}$ dependence is attributed to the fact that in high magnetic fields the scattering-wave states of electrons incident on the conductor from the source contact is spatially separated from the states representing electrons incident on the conductor from the drain contact.

The inelastic scattering length $L_{\rm in}$ is an important physical parameter determining the transport properties of two-dimensional electron gas (2DEG) systems at low temperatures. Extensive studies of $L_{\rm in}$ have been carried out in zero and weak magnetic fields, e.g., via the electron-wave interference effects in the double-slit geometry[1] and the negative magnetoresistance in the weak localization regime.[2]

In high magnetic fields, however, experimental works of $L_{\rm in}$ were limited to those of temperature scaling[3–5] that studied temperature exponents of $L_{\rm in}$. In our previous work,[6] we studied *size scaling*[7] of the integer quantum Hall (IQH) transition and successfully determined absolute sizes of $L_{\rm in}$. To achieve a deeper understanding of inelastic scattering processes, it is important to study the electron-energy dependence of $L_{\rm in}$.

The simplest and most widely applied method of tuning electron energy is to elevate the lattice temperature $T_{\rm L}$. An alternative approach is the control of the source-drain voltage $V_{\rm SD}$. In zero magnetic field, it is known that increasing $V_{\rm SD}$ has an effect equivalent to that of elevating $T_{\rm L}$, viz., increasing $V_{\rm SD}$ strongly decreases $L_{\rm in}$, which can be interpreted as a consequence of the rise in the effective electron temperature.[1] Here, we show that the influence of increasing $V_{\rm SD}$ is surprisingly small compared to the effect of elevating $T_{\rm L}$, and we argue that in high magnetic fields the physical implication of increasing $V_{\rm SD}$ on the inelastic scattering processes is distinctly different from that of elevating $T_{\rm L}$. Several groups performed current-scaling experiments earlier and derived exponents that are different from those with temperature scaling. The difference has led the authors to assume that the effect of $V_{\rm SD}$ is suppressed by energy-relaxation processes inside the conductor.[8–10]

Here, we present a different interpretation and argue that the influence of $V_{\rm SD}$ on the inelastic scattering processes is intrinsically weak in IQH systems. We carry out systematic studies of the $V_{\rm SD}$ dependence as well as of the $T_{\rm L}$ dependence. We argue that the observed robustness of $L_{\rm in}$ against $V_{\rm SD}$ neither comes from energy-relaxation processes inside the conductor nor arises from inefficiency of $V_{\rm SD}$ in generating nonequilibrium electrons in the conductor. From the viewpoint of scattering-theoretic approach,[11–13] we note that in strong magnetic fields the scattering-wave states that are filled by electrons entering the conductor from the (electron-injecting) source contact are spatially separated from the (empty) scattering-wave states that represent electron waves incident on the conductor from the drain contact. We suggest that this strongly suppresses the inelastic scattering processes between the two sets of scattering-wave states, leading to the observed weak dependence of $L_{\rm in}$ on $V_{\rm SD}$.

Samples are standard Hall bars with a Schottky front gate as illustrated in the inset of Fig. 1(a). They are fabricated on an $Al_{0.3}Ga_{0.7}As/GaAs$ heterostructure crystal with a 4.2-K electron mobility of $\mu_{\rm H}=100\ {\rm m^2/V\,s}$ and a sheet electron density of $n_{\rm s}=2.7\times10^{15}\ {\rm m^{-2}}$. The 2DEG regions underneath the gates are regular squares with a side $L=20$, 40, 80, and 160 μm long. Four-terminal measurements are carried out in a ^{3}He-^{4}He dilution refrigerator system at temperatures down to 25 mK. Low-pass filters are used inside the mixing chamber as well as outside the cryostat to eliminate the noise heating. The differential longitudinal resistance, $\partial R_{xx}/\partial V_{\rm G}$

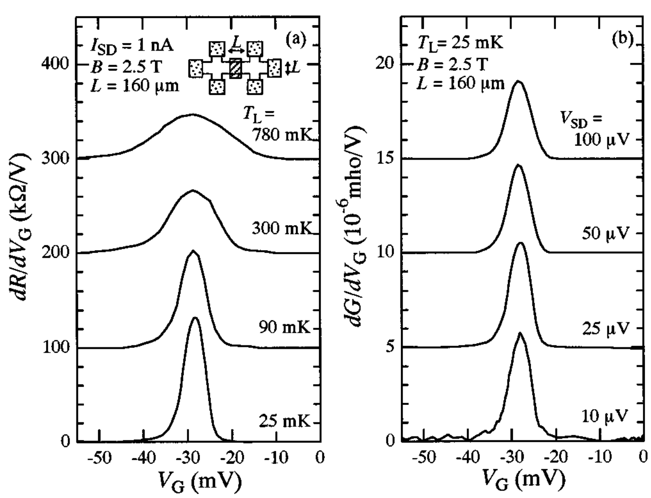

FIG. 1. (a) Differential longitudinal resistance $dR/dV_{\rm G}$ as a function of gate-bias voltage $V_{\rm G}$ for a small source-drain current of $I_{\rm SD}=1$ nA at different lattice temperatures $T_{\rm L}$. The lines are offset for clarity. The inset is a schematic representation of the sample. (b) Differential longitudinal conductance $dG/dV_{\rm G}$ for different source-drain voltages $V_{\rm SD}$ at $T_{\rm L}=25$ mK. The lines are offset for clarity.

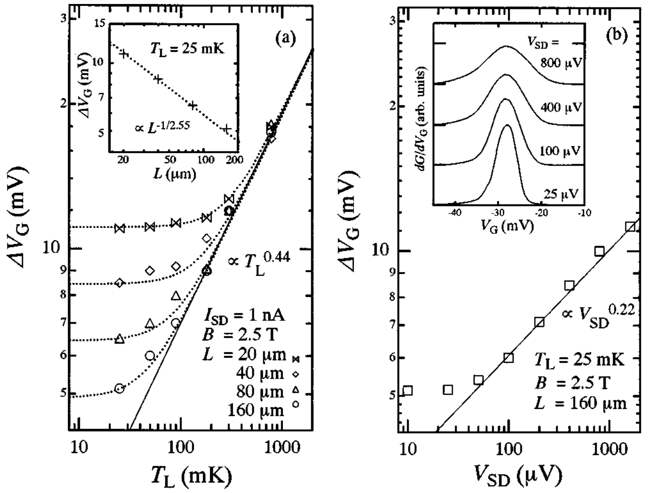

FIG. 2. (a) Transition width ΔV_G against the lattice temperature T_L for different-size samples. The solid line is a fit to the data at elevated T_L's. The dotted lines are theoretically predicted values for individual samples. (See the text and Ref. 15.) The inset shows ΔV_G against sample size L at $T_L = 25$ mK. (b) ΔV_G against the source-drain voltage V_{SD}. The solid line is a fit to the data in a higher-V_{SD} range. The inset shows the transition spectra for the higher-V_{SD} range.

$\propto \partial V_x / \partial V_G$, is studied by applying a dc current of $I_{SD} = 1$ nA and modulating the gate-bias voltage V_G with the peak-to-peak amplitude of $V_{p\text{-}p} = 1$ mV. Similarly, the differential longitudinal conductance, $\partial G / \partial V_G \propto \partial I_{SD} / \partial V_G$, is studied by applying constant dc voltages, V_{SD}'s, and modulating V_G with $V_{p\text{-}p} = 1$ mV.

Figures 1(a) and 1(b) compare the T_L dependence and the V_{SD} dependence of the transition spectrum between IQH states, taken on a sample of $L = 160$ μm. The magnetic field is fixed at $B = 2.5$ T so that the 2DEG regions outside the gate are kept in the IQH state of the Landau-level filling factor of $\nu = 4$, while the 2DEG system underneath the gate undergoes transition from the $\nu = 4$ IQH state to the $\nu = 3$ IQH state as V_G is negatively biased. Figure 1(a) displays the four-terminal differential resistance and shows that the transition width remarkably increases as the lattice temperature T_L is elevated from 25 mK to 780 mK at a constant low bias current of $I_{SD} = 1$ nA. In contrast to the remarkable T_L dependence, Fig. 1(b) shows that the transition width does not increase remarkably as V_{SD} increases up to 100 μV if T_L is fixed at $T_L = 25$ mK.[14] The voltage of $V_{SD} = 100$ μV corresponds to a temperature as high as $T_{eff} = 1200$ mK if the "effective electron temperature (T_{eff})" of nonequilibrium electrons is estimated from the relation

$$k_B T_{eff} = e V_{SD}, \tag{1}$$

where k_B is the Boltzmann constant and e is the unit charge.

Similar features are observed in all the samples of different L's. To suggest below that the observed weak V_{SD} dependence is of an intrinsic origin, we display in Fig. 2(a) the transition width ΔV_G as a function of T_L for different devices, where ΔV_G is defined as the full width at half maximum (FWHM) of each transition spectrum. At elevated temperatures above $T_L = 250$ mK, the transition widths ΔV_G's from different devices agree with one another, forming a straight line with a slope of $T_L^{0.44}$, while at lower T_L's they are split and saturated to sample-specific values. The L dependence of the saturated values at the base temperature of 25 mK is described by $\Delta V_G \propto L^{-1/2.55}$, as shown in the inset of Fig. 2(a). The former characteristics indicate that L_{in} decreases with increasing T_L and becomes smaller than L to serve as an effective sample size at the elevated T_L's.[6] The experimental results at lower T_L's indicate that the conduction is determined by the sample size L because L_{in} exceeds L.[6] The conductors are thus in the coherent regime at the lower T_L's; specifically, we can safely assume that $L_{in} > 160$ μm at $T_L = 25$ mK, as will be explicitly shown later.

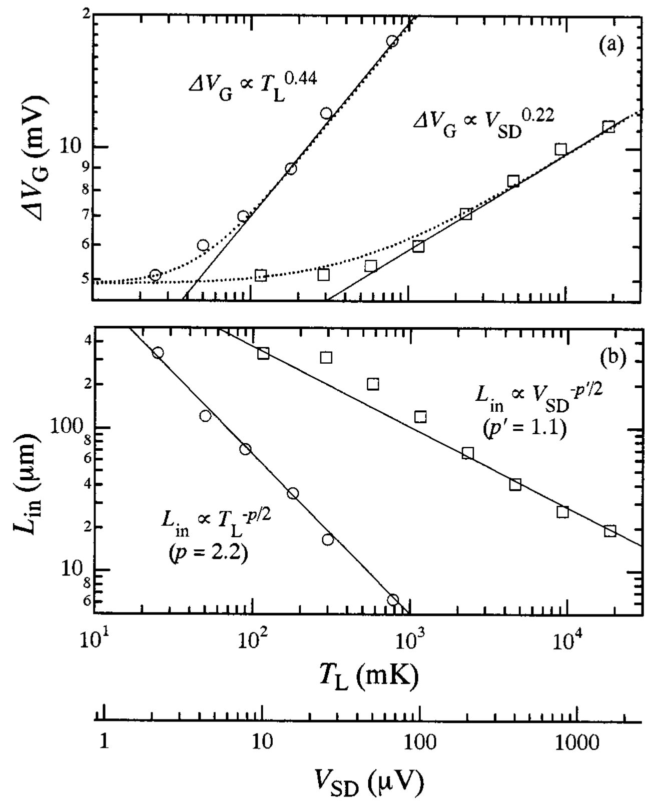

FIG. 3. (a) The transition width ΔV_G against T_L and V_{SD}. The solid lines are fits to the data. The dotted lines are theoretical values predicted by using $L_{in}(T_L)$ in Fig. 3(b). (b) Derived values of the inelastic-scattering length L_{in} against T_L and V_{SD}. The solid lines are fits to the data.

When V_{SD} exceeds 100 μV, ΔV_G eventually starts to increase with increasing V_{SD} with a dependence of $\Delta V_G \propto V_{SD}^{0.22}$, as shown in the inset of Fig. 2(b) for the sample of $L = 160$ μm. Note that the largest value of eV_{SD} or $k_B T_L$ applied in the present experiment is still much smaller than the Landau-level energy spacing $\hbar \omega_c$.

Figure 3(a) compares the V_{SD} dependence (open squares) and the T_L dependence (open circles) of ΔV_G, where the horizontal axis is so chosen that V_{SD} corresponds to T_{eff} through Eq. (1). The data are shown only for the sample of $L = 160$ μm, for it provides the widest range for comparison. However, the results are similar for all the samples. The increases of ΔV_G are well described as $\Delta V_G \propto T^{0.44}$ and $\Delta V_G \propto V_{SD}^{0.22}$, respectively, at higher levels of T_L and V_{SD}.

TABLE I. Values of the T_L exponent p ($L_{in} \propto T_L^{-p/2}$) and the V_{SD} exponent p' ($L_{in} \propto V_{SD}^{-p'/2}$) and the ratio of p/p', determined at different magnetic fields.

B (T)	ν	p	p'	p/p'
3.3	3-2	2.4	1.2	2.0
2.5	4-3	2.2	1.1	2.0
2.0	5-4	1.9	0.91	2.1

We can translate the values of ΔV_G shown in Fig. 3(a) into absolute values of L_{in}, by noting also the data of Figs. 2(a) and 2(b) and applying the analysis discussed in Ref. 6.[15] Figure 3(b) displays the derived values. The exponents p and p' of the T_L dependence and V_{SD} dependence of L_{in} ($L_{in} \propto T_L^{-p/2}, V_{SD}^{-p'/2}$) are determined, respectively, to be $p = 2.2$ and $p' = 1.1$.

We have found that the weak V_{SD} dependence of ΔV_G or L_{in} is common also at different magnetic fields (yielding different IQH transitions). Table I lists the exponents, p and p', obtained at different magnetic fields. Individual values of p and p' are somewhat dependent on magnetic field.[16] We note, however, that the exponents of the V_{SD} dependence, p', are smaller than the exponents of the T_L dependence, p, by a factor very close to 2, $p/p' = 2$, regardless of magnetic field. In additional experiments on a different $Al_{0.3}Ga_{0.7}As/GaAs$ crystal (used in Ref. 6) with $p = 3.0$, we found that p/p' is again close to 2. Thus, the relation $p/p' = 2$ is suggested to be intrinsic to the high-magnetic-field transport.

In order to interpret the experimental results, we argue first that the effects discussed in this work are of an intrinsic origin. Two points are to be made. First, the influence of V_{SD} on the 2DEG system might be apparently suppressed if the current contacts are poor or nonideal.[17–19] However, the possibility of poor contacts is definitely ruled out in the present experiments because (i) the contact resistance was confirmed to be much smaller than the longitudinal resistance of the 2DEG system for every current contact and (ii) additional studies of I_{SD} dependence (taken from the transition spectra obtained at fixed values of I_{SD}) provided results that are similar to those of the V_{SD} dependence described in Figs. 1–3. Second, the extent of V_{SD}-induced nonequilibrium electron distribution may be reduced if energy-relaxation processes are effective in the conductor, viz., T_{eff} may be reduced by the factor of L_E/L as

$$k_B T_{eff} = eE_{SD} L_E = eV_{SD}(L_E/L), \qquad (2)$$

if the energy-relaxation length L_E is smaller than the sample size L, where E_{SD} is an average electric field in the conductor. This was earlier suggested to be the origin of a different exponent of current scaling.[8–10] In our experiments, however, the inelastic scattering length L_{in} is larger than the sample size, $L = 160\ \mu$m, in a range of $V_{SD} < 70\ \mu$V at $T_L = 25$ mK. Noting that the energy-relaxation length L_E must be intrinsically larger than the inelastic-scattering length, L_{in}, we suppose that L_E is much larger than L in our experiments. In our experiments, therefore, the effect of V_{SD} is much weaker than that of T_L in the condition where the energy-relaxation processes cannot be effective. Furthermore, even in the higher-V_{SD} range where $L_{in} < L$, the observed discrepancy between the effects of V_{SD} and of T_L is too large to be accounted for by Eq. (2). For instance, Fig. 3(b) shows that the values of $k_B T_L$ and eV_{SD} at which $L_{in} \approx 20\ \mu$m differ by a factor of $k_B T_L / eV_{SD} \approx 1/60$, whereas the damping factor is at most $L_E/L = L_{in}/L \approx 1/8$. Energy-relaxation processes are thus concluded to be irrelevant to the phenomena discussed here.

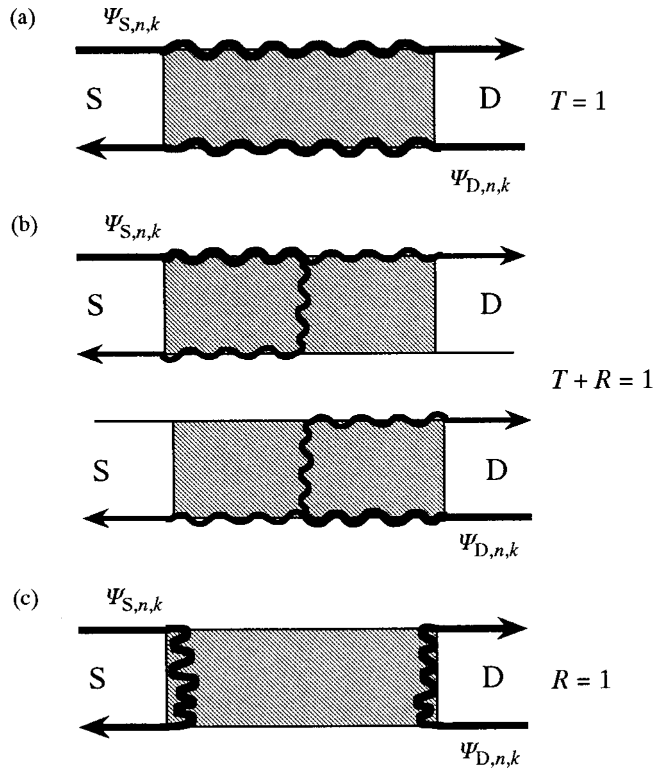

FIG. 4. Schematic representation of $\Psi_{S,n,k}$ and $\Psi_{D,n,k}$ for (a) $T = 1$, (b) $T + R = 1$, and (c) $R = 1$.

In zero magnetic field, L_{in} has been reported to decrease remarkably with increasing V_{SD}, which strongly suggests that the effect of increasing V_{SD} is equivalent to that of elevating T_L if V_{SD} is scaled by Eq. (1).[1] Accordingly, the weak V_{SD} dependence found in the present experiments is likely to be a characteristic of high-magnetic-field phenomena, not observable in the absence of magnetic field.

Let us consider a simplified two-terminal conductor shown in Fig. 4, where a disordered 2DEG region is connected to ideal leads at the opposite ends. Although not shown, the ideal leads are jointed, respectively, to two electron reservoirs with given electrochemical potential μ_S and μ_D. In the presence of transport, $\mu_S > \mu_D$, the electron reservoir on the left serves as the source of electrons and the one on the right as the sink (drain) of electrons. In actual experiments, the 2DEG region underneath the gate, the 2DEG regions outside the gate, and the metallic Ohmic contacts (source and drain), respectively, represent the disordered scattering region, the ideal leads, and the reservoirs. In the absence of inelastic scattering, one can consider scattering-wave states for the conductor, which forms an orthogonal set of eigenstates.[11–13] Each scattering-wave state for a given two-terminal conductor is classified to two groups: In one group, the scattering-wave state $\Psi_{S,n,k}$ describes electron waves that are emitted from the source reservoir, propagate along the ideal lead (on the left) with the mode n (Landau-level index) and the wave number k, enter the disordered region, elastically scatter in the disordered region, and finally leave the disordered region by being transmitted and/or reflected to one and/or both of the ideal leads: In the other group, the scattering-wave state $\Psi_{D,n,k}$ similarly describes electron waves that are emitted from the drain reservoir. We emphasize that a partial reflection (or transmission) described by the scattering-wave states is not a consequence of inelastic scattering. That is, the scattering-wave states $\Psi_{S,n,k}$ and $\Psi_{D,n,k}$ are exact eigenstates of the system in the absence of inelastic scattering processes, which have taken complete account of the effect of elastic scattering processes in the disordered region of the conductor. The scattering-wave states in the first group, $\Psi_{S,n,k}$, are occupied with electrons up to the electrochemical potential of the source reservoir μ_S, while those in the other group, $\Psi_{D,n,k}$, are occupied up to the electrochemical potential of the drain reservoir μ_D, where $\mu_S-\mu_D=eV_{SD}$.

Considering the highest occupied Landau level n and a small energy interval $\mu_D<\epsilon<\mu_S$, an IQH transition is described as follows.[17,20] In the middle of the $\nu=n$ IQH state, $\Psi_{S,n,k}$ and $\Psi_{D,n,k}$ are simply edge states with the transmission probability of $T=1$ as schematically illustrated in Fig. 4(a). As the Fermi level E_F in the disordered region lowers, backscattering[17] takes place, yielding a finite probability of reflection, $R\neq 0$ $(T+R=1)$, as illustrated in Fig. 4(b). When the Fermi level lowers sufficiently, the transmission probability completely vanishes, $T=0$ $(R=1)$, whereby the transition is completed as illustrated in Fig. 4(c).

In the earlier stage of the transition regime where E_F is above the Landau-level center E_C, the transmission coefficient dominates $(T>R)$, and the scattering-wave states may be viewed as edge states that are hybridized with bulk states through random potentials. An average envelope function of the position probability density $|\Psi_{S(D),n,k}|^2$, peaked along one relevant boundary of the conductor, will have an exponential tail penetrating widthwise into the interior region, as illustrated in Fig. 5(a) for the case of $|\Psi_{S,n,k}|^2$. We suppose that the characteristic penetration depth is given by the localization length $\xi(E_F-E_C)$ of bulk states.[21] In the latter half stage of the transition where $E_F<E_C$ $(R>T)$, strong backscattering will take place along the junction between the (entry) ideal lead and the disordered region, and the exponentially decaying penetration of $|\Psi_{S(D),n,k}|^2$ into the interior region takes place lengthwise. We expect again that the characteristic penetration depth is given by $\xi(E_F-E_C)$ as shown in Fig. 5(b). When E_F is close to the level center E_C and the localization length $\xi(E_F-E_C)$ well exceeds the size of the disordered region L, the probability densities of the two groups of scattering-wave states, $|\Psi_{S,n,k}|^2$ and $|\Psi_{D,n,k}|^2$, are peaked, respectively, at the diagonally opposite corners of the disordered region and deeply penetrate both lengthwise and widthwise. We expect, however, that the two groups $|\Psi_{S,n,k}|^2$ and $|\Psi_{D,n,k}|^2$ always avoid each other, being separately distributed in the disordered region as schematically illustrated in Fig. 5(c). [Only when E_F is exactly at E_C does $\xi(E_F-E_C)$ diverge, yielding an appreciable overlap between $|\Psi_{S,n,k}|^2$ and $|\Psi_{D,n,k}|^2$].

The view presented above explains why the transition width decreases with increasing sample size at the limit of low T_L and V_{SD} [Fig. 2(a)]. Furthermore, it distinguishes different roles played by the length and the width of samples in an IQH transition and accounts for relevant experimental results reported in our earlier work.[22]

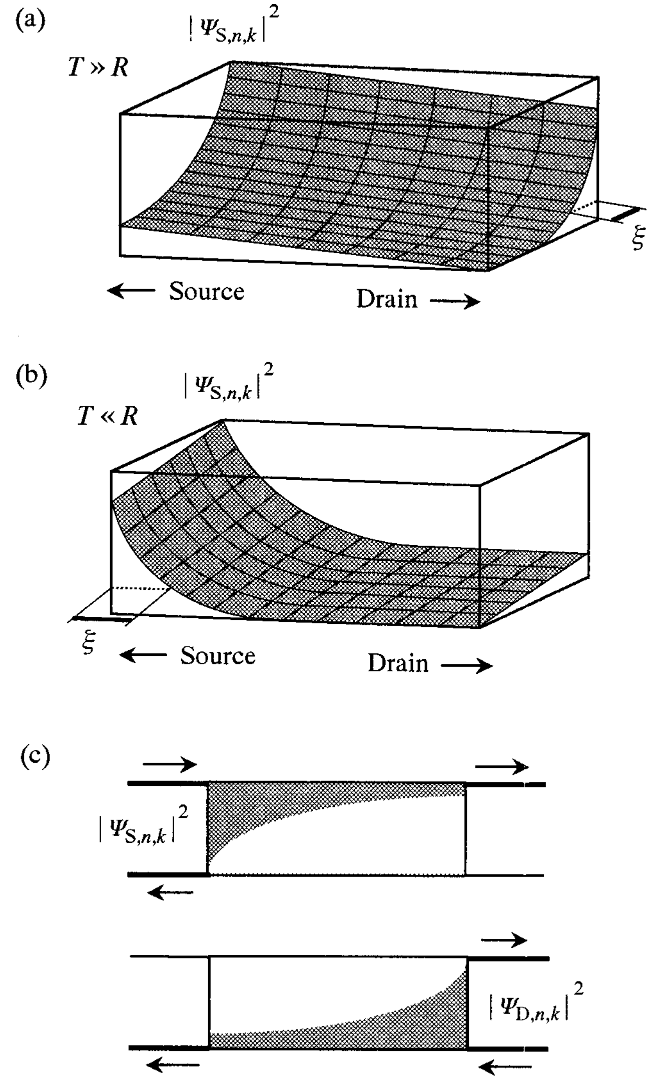

FIG. 5. Schematic representation of an average envelope of the position probability density $|\Psi_{S(D),n,k}|^2$ of scattering-wave states. (a) $|\Psi_{S,n,k}|^2$ for $E_F>E_C$ $(T\gg R)$. (b) $|\Psi_{S,n,k}|^2$ for $E_F<E_C$ $(T\ll R)$. (c) $|\Psi_{S,n,k}|^2$ and $|\Psi_{D,n,k}|^2$ are spatially separated in general, whether $E_F>E_C$, $E_F<E_C$ or $E_F\sim E_C$ $(T\sim R)$.

We can safely assume that the inelastic scattering processes vanish at $T_L=0$ and $V_{SD}=0$.[23] Let us speculate on why the effect of V_{SD} and T_L in introducing the process are markedly different. We should also explain why the effects are similar in the absence of a magnetic field. Our arguments below will be general, being independent of microscopic mechanisms behind the inelastic scattering processes.

Every inelastic scattering process is an event in which an electron is scattered from one scattering-wave state to another. Possible mechanisms causing the scattering include the electron-electron (e-e) interaction, the electron-phonon interaction, and the spin-flip scattering at magnetic impurities. Two electrons are relevant in e-e scattering, while only one electron is relevant in the latter two mechanisms. No matter which particular mechanisms are relevant, we can group any inelastic processes into the following two classes. The ''SD process'' is an inelastic scattering process including scattering between the two different groups of scattering-wave states, $\Psi_{\mathrm{S},n,k}$ and $\Psi_{\mathrm{D},n',k'}$, such as $\Psi_{\mathrm{S},n,k} \rightarrow \Psi_{\mathrm{D},n',k'}$ and $\Psi_{\mathrm{D},n,k} \rightarrow \Psi_{\mathrm{S},n',k'}$. The other, the ''SS process,'' is an inelastic process in which every scattering event occurs within the same group of scattering-wave states, such as $\Psi_{\mathrm{S},n,k} \rightarrow \Psi_{\mathrm{S},n',k'}$ and $\Psi_{\mathrm{D},n,k} \rightarrow \Psi_{\mathrm{D},n',k'}$. (For instance, *e-e* scattering with $\Psi_{\mathrm{S},n,k} \rightarrow \Psi_{\mathrm{D},n',k'}$ and $\Psi_{\mathrm{S},n'',k''} \rightarrow \Psi_{\mathrm{S},n''',k'''}$ is an SD process, while that with $\Psi_{\mathrm{S},n,k} \rightarrow \Psi_{\mathrm{S},n',k'}$ and $\Psi_{\mathrm{D},n'',k''} \rightarrow \Psi_{\mathrm{D},n''',k'''}$ is an SS process.)

When T_L is elevated while V_SD is kept vanishingly small ($\mu_\mathrm{S} \approx \mu_\mathrm{D}$), the two groups of the scattering-wave states, $\Psi_{\mathrm{S},n,k}$ and $\Psi_{\mathrm{D},n,k}$, are occupied with electrons in a similar fashion, with the distribution functions being described by nearly the same, thermally broadened, Fermi functions, f_S and f_D, as schematically shown in Fig. 6(a). By contrast, when V_SD increases while $T_\mathrm{L} \approx 0$, the distribution functions are steplike Fermi functions, f_S and f_D, displaced by eV_SD to each other, as illustrated in Fig. 6(b). Thus, in the energy interval $\mu_\mathrm{D} < \epsilon < \mu_\mathrm{S}$ the group of scattering-wave states $\Psi_{\mathrm{S},n,k}$ originating from the source reservoir is completely occupied with electrons while the other group $\Psi_{\mathrm{D},n,k}$ is empty.

It follows that, in the case of elevating T_L, both SS and SD processes are possible to take place, whereas, in the case of increasing V_SD, SS processes can never occur and only SD processes are possible. (We implicitly assume that $k_\mathrm{B}T_\mathrm{L} = eV_\mathrm{SD}$.) Furthermore, SD processes are expected to be strongly suppressed because the two groups of the scattering-wave states, $\Psi_{\mathrm{S},n,k}$ and $\Psi_{\mathrm{D},n,k}$, are separated at a macroscopic distance. The overlap between the two groups of wave functions, $\propto \exp[-(\xi/L)^2]$, is exponentially small except at exactly the critical point ($E_\mathrm{F} = E_\mathrm{C}$). This explains why L_in is found to be anomalously insensitive to V_SD in the present experiments. SS processes are free from such suppression mechanisms because scattering occurs within the same group of scattering-wave states. The points mentioned above are independent of particular mechanisms responsible for the inelastic scattering processes. We thus have explained why the influence of V_SD on L_in is much weaker than that of T_L.[24]

The discussion above was restricted to the highest occupied Landau level. However, the conclusion is unaltered if lower Landau levels are taken into consideration and arbitrary coupling is admitted between different edge states.

We should note that, in zero magnetic field ($B = 0$), electron wave functions propagating in the opposite directions can have exactly the same profile on a cross-sectional area normal to the propagation direction. Hence, at $B = 0$, the two groups of scattering-wave states, $\Psi_{\mathrm{S},n,k}$ and $\Psi_{\mathrm{D},n',k'}$, substantially overlap one another unless T is nearly zero. Accordingly, V_SD can be as effective as T_L in generating inelastic scattering processes at $B = 0$, which is consistent with the experimental results reported in Ref. 1.

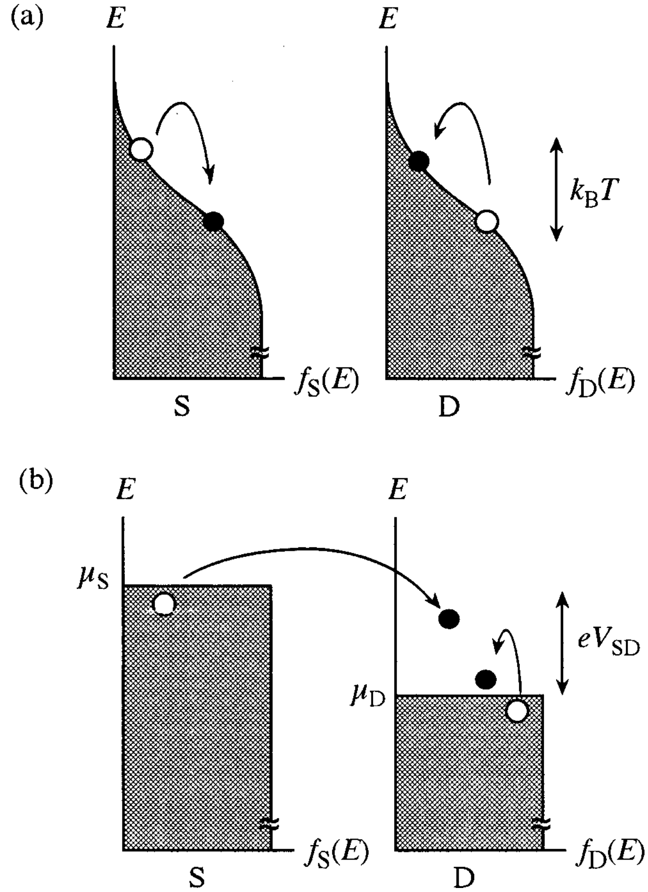

FIG. 6. Schematic representation of the electron distribution functions, f_S and f_D, respectively, for the groups of $\Psi_{\mathrm{S},n,k}$ and $\Psi_{\mathrm{D},n,k}$. Open circles and closed circles denote examples of the initial and the final states, respectively, in inelastic scattering processes. (a) $T_\mathrm{L} > 0$ with $V_\mathrm{SD} = 0$. (b) $T_\mathrm{L} = 0$ with $V_\mathrm{SD} > 0$.

In summary, we have studied the dependence of L_in on V_SD in the 2DEG systems in the IQH regime. L_in derived from the transition spectra between successive IQH plateaus remarkably decreases with increasing T_L. By contrast, the increase of V_SD is much less effective in promoting the inelastic scattering processes. The anomalously weak V_SD dependence of L_in is confirmed to be an intrinsic characteristic of electron systems in high magnetic fields. We interpret these results as a consequence of substantial spatial separation between the two groups of scattering-wave states of electrons that are incident on the conductor from the source and the drain reservoirs.

[1] A. Yacoby, U. Sivan, C. P. Umbach, and J. M. Hong, Phys. Rev. Lett. **66**, 1938 (1991).

[2] For a review, see S. Kawaji, Prog. Theor. Phys. Suppl. **84**, 178 (1985).

[3] H. P. Wei, D. C. Tsui, M. A. Paalanen, and A. M. M. Pruisken, Phys. Rev. Lett. **61**, 1294 (1988).

[4] J. Wakabayashi, M. Yamane, and S. Kawaji, J. Phys. Soc. Jpn. **58**, 1903 (1989).

[5] S. Koch, R. J. Haug, K. von Klitzing, and K. Ploog, Phys. Rev. B **43**, 6828 (1991).

[6] T. Machida, H. Hirai, S. Komiyama, and Y. Shiraki, Phys. Rev. B **54**, 16 860 (1996).

[7] S. Koch, R. J. Haug, K. von Klitzing, and K. Ploog, Phys. Rev. Lett. **67**, 883 (1991).

[8] H. P. Wei, L. W. Engel, and D. C. Tsui, Phys. Rev. B **50**, 14 609 (1994); E. Chow and H. P. Wei, *ibid.* **52**, 13 749 (1995).

[9] S. Koch, R. J. Haug, K. von Klitzing, and K. Ploog, Semicond. Sci. Technol. **10**, 209 (1995).

[10] H. Scherer, L. Schweitzer, F. J. Ahlers, L. Bliek, R. Lösch, and W. Schlapp, Semicond. Sci. Technol. **10**, 959 (1995).

[11] For example, A. Messiah, *Quantum Mechanics* (Wiley, New York, 1965), Vol. II, Chap. 19.

[12] M. Büttiker, IBM J. Res. Dev. **32**, 317 (1988).

[13] S. Komiyama and H. Hirai, Phys. Rev. B **54**, 2067 (1996).

[14] The V_{SD} dependence is represented in terms of conductance (not resistance) in Fig. 1(b). We have confirmed that the dependence is essentially the same also when it is studied in terms of the resistance. A direct comparison between Figs. 1(a) and 1(b) is therefore possible.

[15] By using the values of $L_{\mathrm{in}}(T_{\mathrm{L}})$ shown by the solid line in Fig. 3(b), we can predict, in reverse, values of ΔV_{G} for conductors of arbitrary size L at arbitrary temperature T_{L}. The dotted lines in Fig. 2(a) show the predicted values of ΔV_{G} and their T_{L} dependence for respective samples. The lines reproduce the experimental values well, indicating the consistency of the present analysis.

[16] Nonuniversal values of the exponent p are reported experimentally also in Refs. 5–7, while the universal value of $p=2$ is reported in Ref. 3.

[17] M. Büttiker, Phys. Rev. B **38**, 9375 (1988).

[18] S. Komiyama and H. Hirai, Phys. Rev. B **40**, 7767 (1989).

[19] S. Komiyama, H. Hirai, S. Sasa, and T. Fujii, Solid State Commun. **73**, 91 (1990).

[20] M. Büttiker, in *Nanostructured Systems*, edited by M. Reed, Semiconductors and Semimetals Vol. 35 (Academic Press, New York, 1992), Chap. 4.

[21] See for example, H. Aoki and T. Ando, Phys. Rev. Lett. **54**, 831 (1985).

[22] T. Machida, H. Hirai, S. Komiyama, and Y. Shiraki, Solid-State Electron. **42**, 1155 (1998).

[23] Y. Imry, *Introduction to Mesoscopic Physics* (Oxford University Press, New York, 1997).

[24] Furthermore, we can provide a drastically simplified discussion for the relation $p/p'=2$, as in the following. We take *e-e* scattering as an example. In the case of T_{L} increasing with $V_{\mathrm{SD}}=0$, the rate of scattering with an infinitesimal energy transfer may be roughly scaled by the factor of the combined occupation in the initial and the final states,

$$\begin{aligned} W &= \int\int f_{\mathrm{F}}(\varepsilon_1)[1-f_{\mathrm{F}}(\varepsilon_1)]f_{\mathrm{F}}(\varepsilon_2)[1-f_{\mathrm{F}}(\varepsilon_2)]d\varepsilon_1 d\varepsilon_2 \\ &= (k_B T)^2 \int\int F(y_1)[1-F(y_1)]F(y_2)[1-F(y_2)]dy_1 dy_2 \\ &\propto (k_{\mathrm{B}}T)^2, \end{aligned}$$

where f_{F} is the Fermi function with $F(y)=[1+\exp(y)]^{-1}$ and $y=(\epsilon-\epsilon_{\mathrm{F}})/k_{\mathrm{B}}T_{\mathrm{L}}$. In the case of V_{SD} increasing with $T_{\mathrm{L}}=0$, the factor of the combined occupation is given by

$$\begin{aligned} W &= \int\int f_{\mathrm{S}}(\varepsilon_1)[1-f_{\mathrm{D}}(\varepsilon_1)]f_{\mathrm{D}}(\varepsilon_2)[1-f_{\mathrm{D}}(\varepsilon_2)]d\varepsilon_1 d\varepsilon_2 \\ &= \int\int f_{\mathrm{S}}(\varepsilon_1)[1-f_{\mathrm{D}}(\varepsilon_1)]d\varepsilon_1 \propto eV_{\mathrm{SD}}. \end{aligned}$$

We thus have derived $p/p'=2$.